Structure−Activity Relationship Studies Optimizing the Antiproliferative Activity of Novel Cyclic Somatostatin Analogues Containing a Restrained Cyclic β-Amino Acid†

Martin Sukopp,‡ Richard Schwab,§ Luciana Marinelli,⊥ Eric Biron,‡ Markus Heller,‡ Edit Várkondi,§ Ákos Pap,§ Ettore Novellino,⊥ György Kéri,§ and Horst Kessler*,‡

Lehrstuhl für Organische Chemie und Biochemie II, Technische Universität München, Lichtenbergstrasse 4, 85747 Garching, Germany, Cooperative Research Center, Semmelweis University, Rippl-Ronai u. 37, and Peptide Biochemistry Research Group of Hung. Acad. Sci., H-1062 Budapest, Hungary, and Dipartimento di Chimica Farmaceutica e Tossicologica, Università "Federico II" di Napoli, Via Domenico Montesano, 49 Napoli, Italy

Received June 24, 2004

The cyclic somatostatin analogue cyclo[Pro[1]-Phe[2]-D-Trp[3]-Lys[4]-Thr[5]-Phe[6]] (L-363,301) displays high biological activity in inhibiting the release of growth hormone, insulin, and glucagon. According to the sequence of L-363,301, we synthesized a number of cyclic hexa- and pentapeptides containing nonnatural α- and β-amino acids. The *N*- fluorenylmethoxycarbonyl protected cyclic β-amino acid [1*S*, 2*S*, 5*R*]-2-amino-3,5-dimethyl-2-cyclohex-3-enecarboxylic acid (cβAA), for the replacement of the Phe[6]-Pro[1] moiety of L-363,301, was synthesized in two steps by an enantioselective multicomponent reaction using (−)-8-phenylmenthol as a chiral auxiliary. The resulting peptide cyclo[cβAA[1]-Tyr[2]-D-Trp[3]-Nle[4]-Thr(Trt)[5]] (Trt = triphenylmethyl) shows high antiproliferative effects in an in vitro assay with A431 cancer cells. The same peptide without the Trt group does not reveal any biological activity, whereas L-363,301 and closely related hexapeptides show only minor activity. By comparison of the solution structure of cyclo-[cβAA[1]-Tyr[2]-D-Trp[3]-Nle[4]-Thr(Trt)[5]] with the structure of L-363,301, a nearly perfect match of the βII′-turn region with D-Trp in the $i + 1$ position was observed. The cyclic β-amino acid cβAA is likely needed for the bioactive conformation of the peptide.

Introduction

Somatostatin is a cyclic tetradecapeptide hormone with a disulfide bridge, which was isolated from bovine hypothalami in 1973.[1] First known for its ability to inhibit the release of growth hormone, somatostatin also suppresses the release of many other bioactive molecules (e.g. glucagon, insulin, gastrin, and secretin)[2−4] and mediates tumor cell growth inhibition.[5,6] The biological effects of somatostatin are elicited through a family of G-protein-coupled receptors (GPCR), of which five different forms have been characterized (SSTR1−SSTR5).[7]

Starting from somatostatin, a number of smaller peptidic and nonpeptidic analogues have been synthesized in order to increase receptor subtype selectivity and metabolic stability.[8,9] Among them is the cyclic hexapeptide L-363,301 with the sequence cyclo[Pro[1]-Phe[2]-D-Trp[3]-Lys[4]-Thr[5]-Phe[6]], which was developed by Veber and co-workers.[10−13] This somatostatin analogue shows higher biological activity in inhibiting the release of growth hormone, insulin, and glucagon as well as higher selectivity for the receptor subtype SSTR2. However, its clinical development has been halted due to side effects.[14,15] NMR studies of L-363,301 exhibited a backbone structure which adopts a βII′-turn about residues D-Trp-Lys and an opposite βVI-turn about the Phe-Pro bridging region with a cis amide bond.[16] In the model, the side chains of D-Trp and Lys are in close proximity and the Phe[6] side chain prefers the trans rotamer.[15−17] In general, the side chains of D-Trp, Lys and one further aromatic residue in the right spatial arrangement are important pharmacophoric groups for most of the somatostatin analogues,[18,19] whereas the backbone contributes little to receptor binding in this case.[17,20,21] The latter is also valid for nonpeptidic somatostatin analogues which are highly selective for different receptor subtypes.[22]

Another interesting somatostatin analogue is TT-232 (D-Phe-Cys-Tyr-D-Trp-Lys-Cys-Thr-NH_2) containing seven amino acids, a five-residue ring structure, and a cystein bridge, which was developed by Kéri and co-workers.[23] Also in this somatostatin analogue the biologically important D-Trp-Lys moiety in combination with one aromatic residue (D-Phe or Tyr) is preserved. TT-232 demonstrated potent and tumor-selective antiproliferative activity without an antisecretory action. Several lines of evidence suggest that TT-232 does not cause its effects through somatostatin receptors but by interaction with cytoplasmic and nuclear targets after internalization.[24,25] Another proof is that the binding affinities of TT-232 to all cloned somatostatin receptors are very low compared to that of somatostatin.[26]

Our objective was to develop somatostatin or L-363,301 analogues which are further reduced in ring size and bear mostly hydrophobic, nonnatural residues which in general are used for better pharmacological efficacy and

† This paper is dedicated to the memory of Prof. Murray Goodman, who passed away on June 1, 2004.

* To whom correspondence should be addressed. Telephone: +49-89-289 13300. Fax: +49-89-289 13210. E-mail: Kessler@ch.tum.de.
‡ Technische Universität München.
§ Semmelweis University.
⊥ Università "Federico II" di Napoli.

10.1021/jm049500j CCC: $30.25
Published on Web 03/19/2005

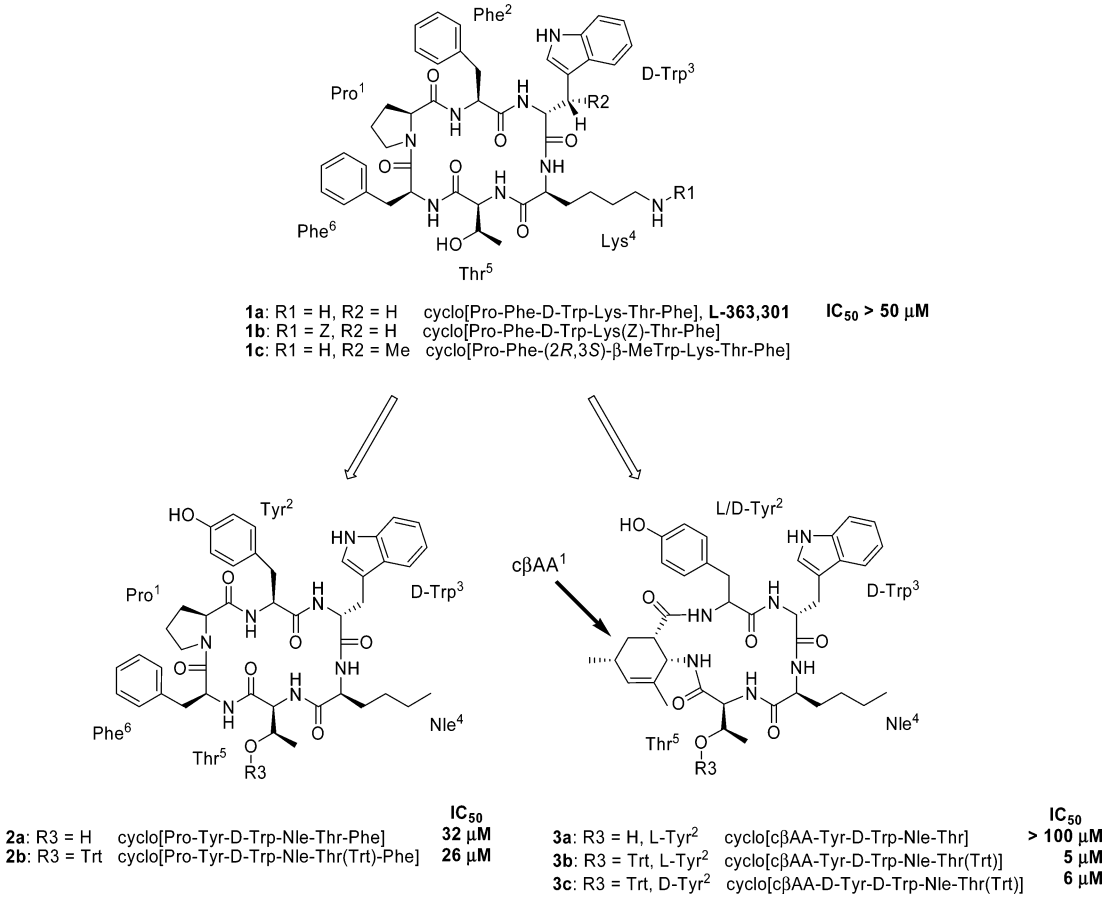

Figure 1. Somatostatin analogues based on L-363,301: Hexa- and pentapeptides with Thr(Trt) residue and/or β-amino acid with IC_{50} values of A431 cancer cell assay.

ADME profiles. Herein, we report the results of our efforts, which led to cyclic pentapeptides with high antiproliferative activity in a cellular assay with A431 human epidermoid carcinoma cells. To explain this finding, we carried out structure−activity relationship (SAR) studies by NMR/modeling techniques.

Results and Discussion

Design and Synthesis of Novel Building Blocks and Target Peptides. To compare the biological activity and structural features of L-363,301 (**1a**) with L-363,301-analogues containing a β-amino acid instead of the Phe-Pro moiety, we synthesized a number of penta- and hexapeptides in which some residues were replaced by homologous amino acids (Figure 1). It was considered that incorporation of a β-amino acid and nonnatural residues (e.g. norleucine) increases the stability against proteases.[27−29] Furthermore, to obtain chemically stable pentapeptide analogues with a defined conformation, the β-amino acid needed to fulfill the following requirements: (1) small, rigid, and easily accessible cyclic structure; (2) hydrophobic and chemical resistant alkane backbone; (3) defined stereochemistry with cis-configuration of amino and carboxylate substituent. A change in the biological activity should be observed just like a previously published, bioactive L-363,301-analogue with trans-configurated β-sugar amino acid instead of the Phe-Pro moiety.[30,31]

The synthesis of cβAA, which was used for incorporation into our somatostatin analogues, is based on a multicomponent reaction published by Beller et al.[32] The series of reaction steps include an aldol reaction of two molecules of aldehyde, the condensation of the amide with the aldol reaction product, isomerization of double bonds, and a Diels−Alder reaction with an acrylate as dienophile in the end (see Scheme 1). By the final cycloaddition reaction the 1-(acylamino)-1,3-butadiene intermediate is removed from the equilibrium in the reaction mixture. The reaction works best using acetic anhydride as water scavenger, camphor sulfonic acid as catalyst, and 2,6-di-*tert*-butyl-4-methylphenol (BHT) for inhibition of acrylate polymerization. Sterically less hindered aldehydes such as propionaldehyde (**4a**) and 3-phenylpropionaldehyde (**4b**) were used in combination with a number of amides, e.g. acetamide (**5a**) and benzylcarbamate (Z-amide) (**5b**). The reaction did not proceed with Fmoc-amide and trifluoroacetamide, but any type of acrylate that we checked yielded the desired product. The reaction was carried out in a pressure reactor at 140−160 °C for 16 h with DMF as solvent, which can be easily removed after the reaction. The products were then isolated by flash chromatography and characterized by NMR and high-resolution mass spectroscopy (HRMS).

The constitution and configuration of the cβAA building block is controlled by several factors. The regioselectivity of the Diels−Alder reaction yields an ortho substituted cyclohexene β-amino acid and the endo selectivity, which leads to an all-syn-substitution pattern, causes the cis-configuration of carboxylate and amide in positions 1 and 2 of cβAA, respectively. The primary structure of the expected α,β,ϵ-substituted

Scheme 1. Synthesis of a Cyclic β-Amino Acid Building Block Using an Enantioselective Multicomponent Reaction

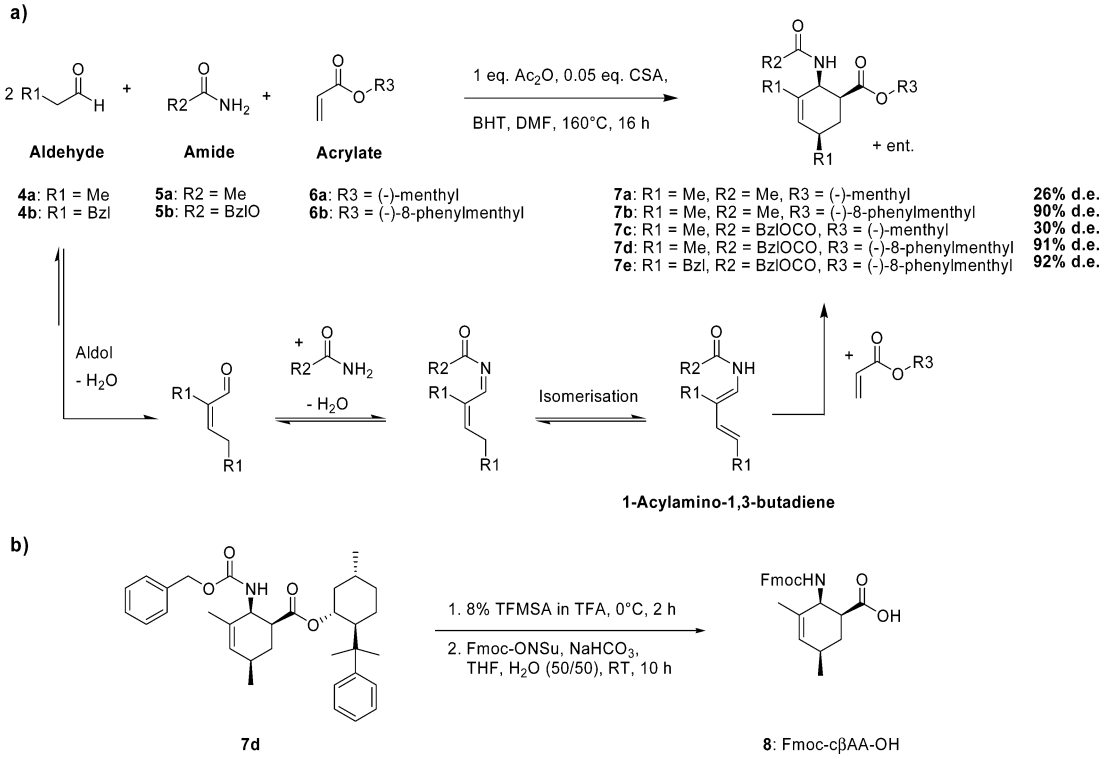

cyclohexene ring could be proven by TOCSY, COSY, and HSQC NMR experiments. Measurements of $^3J_{H,H}$ coupling constants between H^N–H^2 (10.5 Hz) and H^2–H^1 (5.2 Hz) reveal a trans- and a cis-arrangement of the corresponding protons to each other (Figure 2). For control of the enantioselectivity of the Diels–Alder reaction, easily accessible (−)-menthol and (−)-8-phenylmenthol acrylates **6a**,**b** (for synthesis see Experimental Section) were used. It is well-known that in cycloaddition reactions especially the application of (−)-8-phenylmenthol esters favors the formation of nearly only one diastereomer because the phenyl ring of the chiral auxiliary blocks one side of the dienophile by π-interaction.[33,34] This is also reflected by high d.e. (>90%) of the here-described multicomponent reaction of cyclic β-amino acids, whereas the d.e. using (−)-menthol is much lower. The two diastereomers of **7a**–**e** with identical, characteristic $^3J_{H,H}$ coupling constants (see above) could not be separated by chromatography methods, but integration of well-separated ^{1}H NMR peaks (e.g. of H^2) revealed the ratio of both compounds for d.e. calculation.

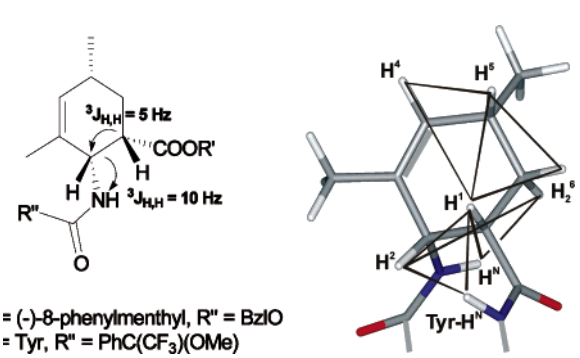

Figure 2. Conformational analysis of the cβAA building block by NMR studies. ROE contacts between protons of **11a,b** are represented by black lines.

For incorporation into peptides by solid-phase synthesis, the amide or carbamate and the auxiliary had to be removed from the products of the multicomponent reaction. Therefore **7d** was treated with 8% trifluoromethanesulfonic acid in anhydrous TFA for 2 h at 0 °C.[35] After removal of acidic solvents by evaporation, the free amino acid was protected with Fmoc-ONSu in a 1:1 mixture of saturated $NaHCO_3$ solution and THF overnight. The resulting Fmoc-cβAA (**8**) was then linked to resin-bound L-tyrosine at the C-terminus and to both enantiomers of Mosher's acid[36] at the N-terminus by standard Fmoc solid-phase peptide synthesis (SPPS)[37] to study the relative and absolute configuration of cβAA more in detail.

The ROESY spectra of **11a**,**b** show very strong peaks, respectively short distances of about 2.5 Å, between H^5–H^1, H^5–H^{6proS}, and H^N–H^{6proR}. Additionally the amide proton of Tyr is in close proximity to H^1 and H^2 in about the same distance as that presented in Figure 2. Thereby, the methylene group CH_2^6 of cβAA points in the same direction as the C^5–CH_3 group to bring the three substituents of the cyclohexene ring in the sterically less hindered equatorial position. Proof for the absolute configuration is given by the differences in chemical shifts ($\Delta = \delta_S - \delta_R$) of the *S*- and the *R*-Mosher amides **11a**,**b**. According to previous investigations positive values have to be right of the H^2–H^N–CO–CF_3 plane of the Mosher amide; negative values will be found in the opposite direction.[36] Especially the strong high-field shifts of +110 and +75 Hz (measurements at 500 MHz) of the C^3–CH_3 group and H^4 confirm the strong anisotropic shielding of the phenyl ring. Other evidence for the absolute configuration is corresponding ROE contacts of Tyr-H^α and H^{6proR} with the methoxy group of the *R*-Mosher amide **11b**, as well as one ROE contact of Tyr-H^α with the phenyl ring of the *S*-Mosher amide **11a** (Figure 3).

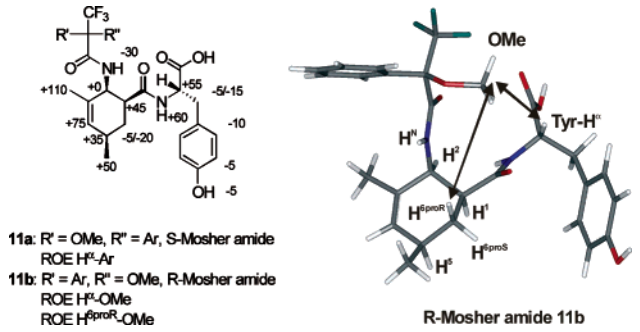

Figure 3. ^{1}H chemical shift differences ($\Delta\delta = \delta_S - \delta_R$) and essential ROE contacts for the Mosher amides of NH_2-cβAA-Tyr-OH. $\Delta\delta$ values are expressed in hertz (500 MHz). The 3D structure of (*R*)-Mosher amide **11b** shows the close proximity of the OMe group to H$^\alpha$ of Tyr. Arrows represent essential ROE contacts.

The target L-363,301 analogues were successfully synthesized via preparation of the linear peptide on solid support and cyclization in solution (for example, see Scheme 2). Synthesis commenced with TCP resin loaded with side chain unprotected D- or L-Tyr. The Fmoc-Tyr TCP resin **9** was allowed to react with 1.8 equiv of **8** using TBTU/HOBt/DIEA in NMP after deprotection of the Fmoc group with 20% piperidine in NMP. The peptide chain was then assembled by consecutive cleavage steps of Fmoc groups, and additions were done using the same coupling reagents and 3 equiv of Fmoc amino acid, respectively. Thereby the hydroxyl group of Thr was protected by a Trt ether, and the D-Trp did not need side chain protection. Since the Trt ether can be removed easily under acidic conditions, the cleavage of the linear peptide from the TCP resin was achieved under very mild conditions with acetic acid in TFE and DCM (2/1/6, v/v/v) after removal of the last Fmoc group from the N-terminal residue. The resulting crude peptide was cyclized in dilute DMF solution in the presence of PyBOP, HOBt, and collidine. Racemization during ring closure of about 10−20% of the C-terminal amino acid could be observed due to sterical hindrance of the Trt group. Target peptides with Thr(Trt) **3b**,**c** were purified by RP-HPLC not adding TFA to the mobile phase in order to prevent cleavage of the Trt group. For fully deprotected cyclic peptides **2a** and **3a**, nonpurified intermediates **2b** and **3b** were treated with 2% TFA and TIS in DCM for 1 h before final HPLC purification. All target peptides exhibit a very low solubility in water due to their hydrophobic residues, especially the ones with a Thr(Trt) moiety.

Biological Results. Human A431 epidermoid carcinoma cells were used for evaluating the antiproliferative efficacy of peptides **1a**, **2a**,**b**, and **3a**−**3c**. Thereby, comparison of drug-treated cells with untreated cells revealed no necrotic side effects after 6 h, indicated by the unchanged proliferation of both cell cultures after staining with methylene blue. However, cells treated with different amounts of some of the peptides showed significant reduced proliferation after 48 h compared to the negative controls. Cycloheximide, used as a positive control, exhibited the same behavior. The IC_{50} values were generated from the growth (%) to concentration (μM) graphs and are given in Figure 1.

Surprisingly, the reference peptide **1a** (>50 μM) was biologically less active in this assay than the two peptides **3b**,**c**, with IC_{50} values of 5 and 6 μM, respectively. This behavior might indicate a different mode of action that is not directly mediated by the somatostatin receptors SSTR2 and SSTR5. Furthermore, the two hexapeptides **2a**,**b** that were designed to explore the structural transition from L-363,301 (**1a**) to the most active peptides **3b**,**c** exhibit biological activities of 32 and 26 μM, respectively. It seems that already the exchange of Lys^4 to Nle^4 and Phe^2 to Thr^2 (**2a**) has a positive effect on the biological activity that can be slightly improved by adding a Trt group to the Thr^5 residue (**2b**). The greatest improvement in activity is achieved by introduction of cβAA^1 (**3b**) instead of the Phe^6-Pro^1 moiety, while shifting from a hexa- to an extended pentapeptide. Additionally, the biological activity of **3b**,**c** is increased by approximately 50% compared to a similar peptide with a trans-configurated sugar amino acid instead of cβAA (cis-configuration).[30,31]

Two further assumptions can be drawn from the results of biological testing of compounds **3a**−**c**. It seems that the absence of trityl group in peptide **3a** results in the complete loss of antiproliferative activity (IC_{50} > 100 μM). Therefore, the trityl group might function as an important pharmacophoric group. Another fact is that the change of the Tyr^2 configuration in peptides **3b**,**c** has only a minor influence on the activity of the peptides. Possible reasons for these findings will be discussed in the next paragraph dealing with the structures of the tested peptides.

Structural Analysis of L-363,301 Analogues. Structurally relevant ^{1}H and ^{13}C chemical shifts of L-363,301 analogues **2a,b** and **3a**−**c** were assigned by TOCSY, HMQC, and DQF−COSY experiments in DMSO-d_6 at 300 K. Additionally, $^3J_{H,H}$ coupling constants of amide protons and H$^\beta$-protons were extracted from 1D spectra, as well as temperature gradients of amide protons in the range of 295−320 K. For structural comparison, NMR data and 3D structures of **1a** and two analogues **1b**,**c** were taken from refs 12, 16, 18, and 19.

First structural similarities among the examined peptides were revealed by comparison of chemical shifts, coupling constants, and temperature gradients of amide protons (Table 1). It is shown that the H^N chemical shifts of peptides **1a**−**c**, which differ only in the methylation of a D-Trp side chain or in the attachment of a Lys side chain protecting group, are nearly identical. This is reflected by a good match of secondary structures published by Goodman et al.[19] and our group.[16] Especially, the βII′-turn of the D-Trp-Lys-Thr moiety is highly conserved which is also expressed by an exact match of H^N coupling constants. A strong β-turn hydrogen bond is indicated by a very low temperature gradient of the Thr amide proton of approximately 0 ppb/K.[38]

Since chemical shifts and temperature gradients of amide protons (Lys^4/Nle^4 and Thr^5) as well as the coupling constants of D-Trp^3 and Lys^4/Nle^4 (highlighted in italic characters in Table 1) exhibit strong consistency, it can be assumed that also the secondary structures, especially the β-turn region, of the listed peptides are very much the same. Corresponding values of amino acids flanking the β-turn region show larger differences due to substitutions of residues and changes in conformation, especially by introducing the cβAA residue.

Scheme 2. Synthesis of L-363,301 Analogues with Thr(Trt) Residue[a]

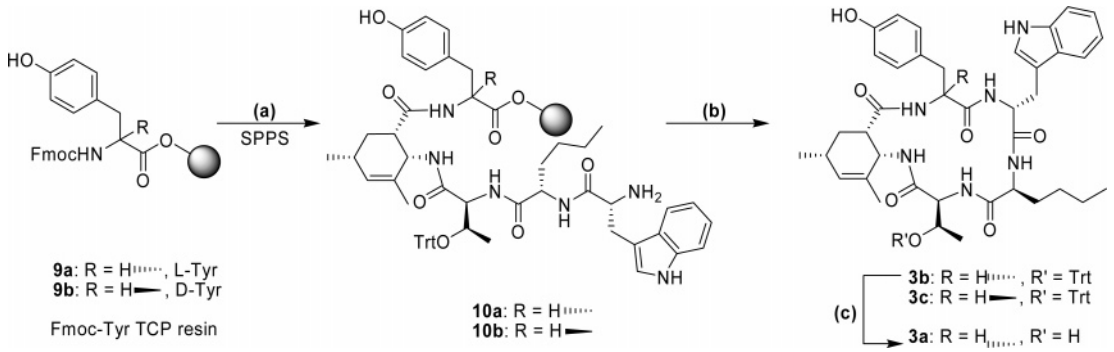

[a] (a) (i) 20% piperidine in NMP, (ii) 1.8 equiv of Fmoc-cβAA-OH, TBTU, HOBt, DIEA, NMP, (iii) 20% piperidine in NMP, (iv) Fmoc-Thr(Trt)-OH, TBTU, HOBt, DIEA, NMP, (v) 20% piperidine in NMP, (vi) Fmoc-Nle-OH, TBTU, HOBt, DIEA, NMP, (vii) 20% piperidine in NMP, (viii) Fmoc-Trp-OH, TBTU, HOBt, DIEA, NMP, (ix) 20% piperidine in NMP; (b) (i) AcOH, TFE, DCM (2/1/6), RT, 1 h, (ii) 1.2 equiv of PyBOP, HOBt, collidine, DMF, RT, 16 h, (iii) purification by RP-HPLC (without TFA); (c) (i) 2% TFA in DCM, TIS, 1 h, (ii) purification by RP-HPLC.

Table 1. Chemical Shifts, $^3J_{H^N,H^a}$ Coupling Constants, and Temperature Gradients of Amide Protons of Cyclic Somatostatin Analogues **1a**−**c**, **2a**,**b**, and **3a**,**b**[a]

	peptide	Phe^2/Tyr^2	D-Trp^3	Lys^4/Nle^4	Thr^5	cβAA^1/Phe^6
chemical shift (ppm)	**1a**	7.20	8.40	*8.67*	*6.96*	8.30
	1b	7.21	8.41	*8.65*	*6.95*	8.30
	1c	7.42	8.41	*8.65*	*6.95*	8.30
	2a	7.15	8.31	*8.59*	*6.95*	8.28
	2b	7.00	8.25	*8.49*	*6.79*	7.87
	3a	7.82	8.06	*8.62*	*7.03*	7.44
	3b	7.84	8.16	*8.61*	*6.86*	7.53
	3c	7.96	8.56	*8.17*	*6.90*	7.60
$^3J_{H^N,H^a}$ (Hz)	**1a**	*b*	*7.8*	*7.0*	7.4	4.9
	1b	6.4	*8.3*	*7.2*	7.5	6.0
	1c	6.0	*8.2*	*7.1*	7.5	4.5
	2a	*b*	*8.2*	*7.3*	7.4	5.4
	2b	*b*	*8.2*	*7.3*	5.8	6.5
	3a	8.5	*7.5*	*7.3*	5.0	9.7
	3b	8.7	*7.7*	*7.3*	5.2	9.9
	3c	7.8	*6.2*	*6.4*	6.4	9.6
$-\Delta\delta/\Delta T$ (ppb/K)	**1a**	1.6	5.1	*5.4*	*0.3*	2.8
	1b	1.0	4.8	*5.0*	*0.2*	2.8
	1c	5.4	6.0	*5.4*	*−0.7*	4.8
	2a	1.0	5.8	*5.8*	*0.0*	2.8
	2b	0.3	5.5	*5.4*	*0.3*	−0.2
	3a	4.2	8.5	*6.7*	*−0.9*	5.3
	3b	4.4	9.2	*4.9*	*−1.0*	13.1
	3c	4.4	3.6	*1.2*	*0.0*	9.2

[a] The values of peptides **1a**−**c** were taken from refs 12,16,18,and 19. [b] No coupling constant available due to signal overlap.

Another important observation is that by removal of the trityl group from the side chain of Thr (e.g. see **2a/b** and **3a/b**) the order of chemical shifts, the coupling constants, and probably also the backbone structure do not change to a larger extent. In contrast to this, the inversion of D-Tyr^2 into L-Tyr^2 in peptide **3c** indicates stronger conformational changes reflected by substantial differences in chemical shifts and coupling constants of the amide protons compared to **3b**. Nevertheless, the amide proton of Thr^5 remains to be internally oriented (e.g. by a hydrogen bond) indicated by a low-temperature gradient of 0 ppb/K.

For a detailed structural comparison with L-363,301, the NMR structure of cyclo[cβAA-Tyr-D-Trp-Nle-Thr(Trt)] (**3b**) was determined using a combined approach of metric matrix distance geometry (DG) calculations and molecular dynamics (MD) simulations based on 35 distance restraints obtained from ROESY experiments with mixing times of 250 ms (0.8 mg of peptide in 0.5 mL of DMSO-d_6 at 300 K) following standard strategies.[39] The prochiral methylene protons of cβAA-H^6 and Tyr-H$^\beta$ could be stereospecifically assigned on the basis of ROE values and $^3J_{H,H}$ coupling constants. The NMR data and the results from DG calculations of **3b** revealed a rigid and well-defined structure of the backbone, showing a slightly distorted βII′-turn with D-Trp^3 in the $i + 1$ position (Figure 4). The MD calculations were performed first by using the experimental restraints followed by a free dynamic simulation in an explicit solvent box filled with DMSO.[40] The rmsd over all backbone atoms between the average structures from restrained and free MD simulations is only 0.13 Å. Small violation of distance restraints (<0.2 Å) during MD calculations was observed for the Thr backbone representing partial flexibility of this part of the cyclopeptide. Preferred conformations for the side chains of Tyr^2, D-Trp^3, Nle^4, and Thr^5 were also obtained by restrained DG in combination with $^3J_{H\alpha,H\beta}$ coupling constants. As shown in Figure 4, the bulky γ-methyl group of Thr^5 points in the same direction as the amide proton of Thr and shields the latter from surrounding DMSO. In combination with the internal β-turn hydrogen bond between H^N-Thr^5 and CO-Tyr^2 which is populated to a degree of 31% during restrained MD [the

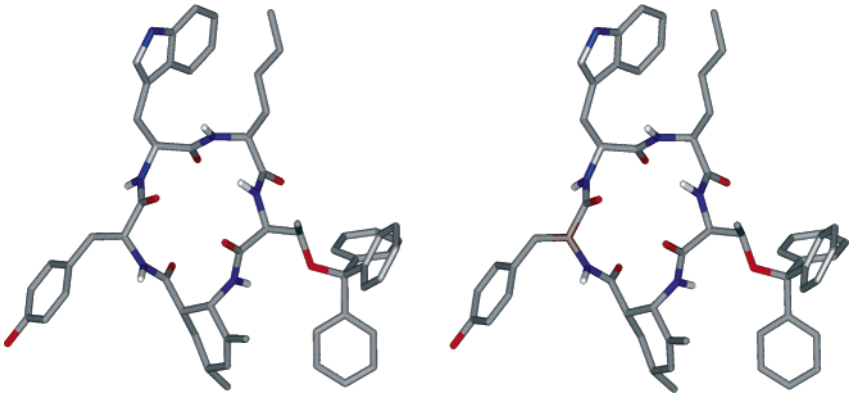

Figure 4. Stereoview of cyclo[cβAA-Tyr-D-Trp-Nle-Thr(Trt)] (**3b**) of the most representative structure in DMSO obtained by MD simulations.

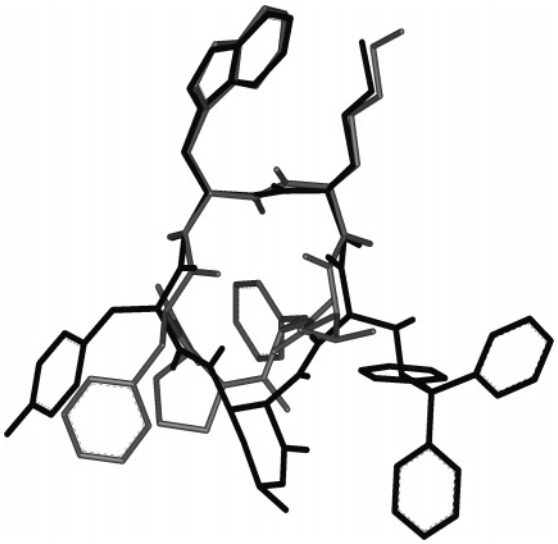

Figure 5. Superimposition of the NMR solution structures of cyclo[cβAA-Tyr-D-Trp-Nle-Thr(Trt)] (**3b**; black) and L-363,-301 (**1a**; gray). Only heavy atoms and amide hydrogens are displayed for clarity.

tolerance of the angle was set to 70°, while the tolerance of the distance was set to 3.2 Å], this might be the reason for an extremely low temperature gradient of $-\Delta\delta/\Delta T = -1.0$ ppb/K of the Thr amide proton. Other protons such as H^N-cβAA^1 and H^N-D-Trp^3 are fully surrounded by solvent molecules according to their temperature gradient of 13.1 and 9.2 ppb/K, respectively. For the Tyr side chain a strongly preferred gauche$^+$ conformation can be stated on the basis of a distinct stereospecific assignment of H^β protons. In contrast to the latter, the side chains of D-Trp^3 and Nle^4 show higher conformational freedom during DG calculations, but a close, parallel orientation of both side chains has to be preferred since the ϵ- and γ-protons of the Nle chain are shifted to higher field and due to a ROE peak between H^ϵ-Nle and H^{6Ar}-D-Trp with a corresponding distance of 4.3 Å. Conformation and absolute configuration of the cβAA residue is in accordance with the ROE data of **3b**, coupling constants of H^2 (9.5 and 3.6 Hz), and the structure of Mosher amide **11**.

Structural comparison of **3b** with **1a** (Figure 5) reveals a good fit of the β-turn backbone of both peptides with a rmsd of 0.21 Å (based on Ca atoms of Tyr, D-Trp, Nle/Lys, and Thr). It seems that the β-turn motive that appears in a number of somatostatin analogues (with D-Trp in the $i + 1$ position) is also a key element for the biological activity of **3b**. Interestingly, cβAA is able to shorten and substitute the Phe-Pro moiety of L-363,-301 while having the same structural effect of a βVI-turn on the rest of the cyclopeptide. This means that the D-amino acid can keep its strong conformational influence on the cyclopeptide and the βII′-turn remains in its original position. Thereby the cis-configuration of amino and carboxylate substituents of cβAA seems to fit the conformational requirements for high activity better than a β-amino acid building block with a trans-configuration (2-fold increase of activity).

Similarities in orientation are also found for the side chains of D-Trp and Nle/Lys, shown in Figure 5, whereas significant structural differences emerge for the backbone and side chains of Tyr/Phe^2 and Thr^5 by the influence of cβAA. Especially, the voluminous trityl group of Thr^5 occupies a huge space besides the Thr residue (right side of Figure 5) which is not populated by the Phe^6 side chain of L-363,301 in its most favored NMR conformation. Nevertheless, superimposition of the Trt group of Thr^5 in **3b** and the side chain of Phe^6 in L-363,301 could be obtained if the side chain of Phe^6 would switch from the preferred trans to a gauche conformation by induced fit into the target receptor. From biological and structural results it can be assumed that an aromatic residue in the region of the trityl group next to Thr^5 is essential for antiproliferative activity of L-363,301 analogues. L-363,301 itself seems to show much lower activity since the only aromatic moiety Phe^6 that might fit the pharmacophoric requirements does not prefer the right spatial arrangement. Compared to **3b**, the lower biological activity of peptide **2b** with only a Phe-Pro moiety instead of cβAA also indicates this finding. Therefore cβAA seems to be needed for the correct spatial arrangement of the Thr(Trt) side chain.

In contrast to the aromatic residue next to the Thr^5 residue, the Tyr/Phe^2 residue opposite of Thr^5 seems not to have importance for the biological activity of **3b**. This can be suspected from the fact that the side chain orientations of Tyr^2 or Phe^2 in Figure 5 differ substantially in the C^α–C^β vector. Previously Goodman et al. have shown that conformational changes of Phe^2 by side chain methylation did not influence the biological acitivity of L-363,301 toward the somatostatin receptor, whereas methylation of the more sensitive Phe^6 residue mostly yielded inactive peptides.[18] Here, we observe that the switch from L-Tyr (peptide **3b**) to D-Tyr (peptide **3c**)

changes the conformation of the cβAA-Tyr moiety heavily (see chemical shifts, coupling constants, and temperature gradient of amide protons), while keeping the antiproliferative efficacy. An explanation for this observation could be that only the conformation of the pharmacologically less important cβAA-Tyr part of the β-turn changes but not the conformation of the essential D-Trp-Nle-Thr(Trt) moiety. Structural investigations of **3c** by NMR and modeling calculations confirm this (data not shown). The finding that only two aromatic residues (D-Trp and Thr(Trt) in the case of **3b**) are required for GPCR binding is in accordance with many examples in the literature, e.g. nonpeptidic somatostatin antagonists, enkephalin analogues, and urotensin II analogues.[22,41,42] The fact that peptide **3b** is much more potent than L-363,301 in the cellular assay might point to a biological mode of action that is not dominated by the somatostatin receptors such as that assumed in the case of TT-232.[26,43] Another indication for this finding is that the Lys residue, which is present in all active somatostatin analogues, can be replaced by Nle without loss of activity in the cellular assay.

Conclusion and Outlook

The peptide cyclo[cβAA-Tyr-D-Trp-Nle-Thr(Trt)] (**3b**) that was designed starting from the somatostatin analogue L-363,301 (**1a**) showed very good antiproliferative activity on A431 cells in a cellular assay without necrotic side effects. NMR/modeling together with SAR studies revealed that the structural feature of a βII′-turn about the D-Trp-Lys/Nle moiety, which is found in a number of somatostatin analogues, is also preserved in **3b**. The rigid conformation of **3b** is mainly determined by the D-Trp residue and cyclic β-amino acid (cβAA) that was synthesized by an enantioselective multicomponent reaction. This cyclic β-amino acid seems to play an important role for the orientation of Thr^5 side chain of peptides bearing a biologically important Trt group. The stereochemistry of the Tyr^2 residue does not seem to play an important role for biological activity because both enantiomers can be used without major differences in activity.

Compound **3b** turns out to be an interesting lead in the development of biologically active peptides featuring nonnatural building blocks, reduced number of residues, and increased hydrophobicity. Its defined structure−activity relationship provides important information about pharmacophoric groups and their orientation for further development of antiproliferative drugs for cancer treatment.

Experimental Section

General Methods. Trityl chloride polystyrol (TCP) resin (0.94 mmol/g) was purchased from PepChem. Coupling reagents and amino acid derivatives were purchased from Advanced ChemTech, Perseptive Biosystems GmbH, Neosystem, and PurChem. All other reagents and solvents were purchased from Merck−Schuchardt, Lancaster, Aldrich, and Fluka and were used as received. The solvents ethyl acetate, diethyl ether, methanol, and *n*-hexane were distilled before use. Standard syringe techniques were applied for transferring dry solvents. Reactions on solid support were performed in filter columns (5 and 10 mL) from Abimed. Melting points (mp) were determined on a Büchi 510 apparatus and were uncorrected. ^{1}H spectra were obtained in $CDCl_3$ or DMSO-d_6 as solvent and internal reference on a Bruker DMX500 spectrometer. Chemical shifts (δ) are reported in parts per million (ppm), and coupling constants (J values) are given in hertz (Hz). The following abbreviations were used to explain the multiplicities: s, single; d, doublet; t, triplet; q, quartet; dd, doublet of doublets; dt, doublet of triplets; m, multiplet; b, broad. Thin-layer chromatography was performed on silica gel 60 F_{254} plates from Merck. Flash chromatography was performed on silica gel 60 (230−400 mesh ASTM) from Merck. RP-HPLC analyses and separations were conducted on Amersham Pharmacia Biotech instruments using Omnicrom YMC columns (analytical, 4.6 mm × 250 mm, 5 μm C_{18}, 1 mL/min; semipreparative, 20 mm × 250 mm, 10 μm C_{18}, 8 mL/min) with different 30 min linear gradients from water (0.1% TFA) and CH_3CN (0.1% TFA) and detection at 220 nm. Mass spectra (ESI) were performed on a LCQ Finnigan instrument and high-resolution mass spectra (HRMS) on a Finnigan MAT-8200 instrument.

Synthesis of Intermediates and β-Amino Acids. (a) (−)-Menthyl Acrylate (6a). To a solution of (−)-menthol (7.81 g, 0.05 mol) in 50 mL of THF (dry) first acrylic acid chloride (4.85 mL, 0.06 mol) and then triethylamine (10.5 mL, 0.075 mol) were added under argon atmosphere at 0 °C and stirred for 2 h at the same temperature. After acidification with 2 N buffered acetate solution (pH 4) and evaporation of the THF under reduced pressure, the aqueous mixture was extracted with EtOAc (3 × 100 mL). The combined organic layers were dried over $MgSO_4$, and the solvent was evaporated under reduced pressure. Distillation (high vacuum < 1 mbar) of the raw product afforded **6a** as a colorless liquid (6.4 g, 0.03 mol, 61%): ^{1}H NMR ($CDCl_3$) δ 6.38 (dd, 1H, J = 1.5 and 17.4 Hz, CH^1H^2-acrylate), 6.11 (dd, 1H, J = 10.5 and 17.4 Hz, CH-acrylate), 5.79 (dd, 1H, J = 1.4 and 10.3 Hz, CH$^1H^2$-acrylate), 4.76 (m, 1H, C^{1}H), 2.04/1.02 (2 × m, 2H, C^{6}H$_2$), 1.87 (m, 1H, CH-(CH$_3$)$_2$), 1.70/1.09 (2 × m, 2H, C^{3}H$_2$), 1.70/0.89 (2 × m, 2H, C^{4}H$_2$), 1.51 (m, 1H, C^{5}H), 1.42 (m, 1H, C^{2}H), 0.91 (d, 3H, J = 6.9 Hz, C^5−CH$_3$), 0.89/0.77 (2 × d, 6H, J = 7.0 Hz, C−(CH$_3$)$_2$); ^{13}C NMR ($CDCl_3$) δ 165.8 (CO), 130.3 (CH_2-acrylate), 129.2 (CH-acrylate), 74.6 (C^1), 47.4 (C^2), 41.0 (C^6), 34.6 (C^4), 31.6 (C^5), 26.7 (C-(CH$_3$)$_2$), 23.8 (C^3), 22.4 (C^5-CH$_3$), 20.9/16.7 (C−(CH$_3$)$_2$); RP-HPLC t_R = 21.2 (50−100%).

(b) (−)-8-Phenylmenthyl Acrylate (6b). To a solution of (−)-8-phenylmenthol (5.0 g, 21.6 mmol) in 40 mL of THF (dry) first acrylic acid chloride (2.2 mL, 27.2 mmol) and then triethylamine (5.3 mL, 38.3 mmol) were added under argon atmosphere at 0 °C and stirred for 2 h at the same temperature. After acidification with 2 N buffered acetate solution (pH 4) and evaporation of the THF under reduced pressure, the aqueous mixture was extracted with EtOAc (3 × 100 mL). The combined organic layers were dried over $MgSO_4$, and the solvent was evaporated under reduced pressure. Flash chromatography (EtOAc/*n*-hexane, 1/4, v/v) of the raw product afforded **6b** as a colorless oil (4.5 g, 15.8 mmol, 73%): R_f = 0.40 (*n*-hexane); ^{1}H NMR ($CDCl_3$) δ 7.29−7.22 (m, 4H, Ar), 7.10 (t, 1H, J = 6.7 Hz, Ar), 6.01 (dd, 1H, J = 14.2 and 4.6 Hz, CH^1H^2-acrylate), 5.59 (dd, 1H, J = 10.5 and 20.1 Hz, CH-acrylate), 5.57−5.56 (m, 1H, CH$^1H^2$-acrylate), 4.88 (m, 1H, C^{1}H), 2.08−2.02 (m, 1H, C^{2}H), 1.93/0.99 (2 × m, 2H, C^{6}H$_2$), 1.68/1.11 (2 × m, 2H, C^{3}H$_2$), 1.64/0.88 (2 × m, 2H, C^{4}H$_2$), 1.49 (m, 1H, C^{5}H), 1.31 (s, 3H, C−CH$_3$), 1.23 (s, 3H, C−CH$_3$), 0.87 (d, 3H, J = 6.6 Hz, C^5-CH$_3$); ^{13}C NMR ($CDCl_3$) δ 165.4 (CO), 151.6 (Ar), 129.9 (CH_2-acrylate), 128.9 (CH-acrylate), 128.0 (Ar), 125.4 (Ar), 125.0 (Ar), 74.6 (C^1), 50.5 (C^2), 41.6 (C^6), 39.7 (C$_q$), 34.6 (C^4), 31.3 (C^5), 27.6 (C-CH$_3$), 26.7 (C^3), 25.4 (C-CH$_3$), 21.6 (C^5-CH$_3$); RP-HPLC t_R = 23.6 (50−100%).

General Procedure for Multicomponent Reaction (7a−e). Aldehyde **4** (10 mmol), amide **5** (10 mmol), acrylate **6** (3 mmol), 1.5 mL of acetic anhydride (16 mmol), 8 mL of DMF, 0.05 g of camphorsulfonic acid, and 0.05 g of 2,6-di-*tert*-butyl-4-methylphenol (BHT) are placed in a pressure reactor and stirred for 16 h at 140−160 °C. Afterward, volatile compounds are removed by evaporation under high vacuum. Flash chromatography (EtOAc/*n*-hexane) of the raw product affords **7** as a colorless oil (approximately 30% yield).

(a) [1*S*, 2*S*, 5*R*]-2-(Acetylamino)-3,5-dimethylcyclohex-3-enecarboxylic Acid (−)-Menthyl Ester (7a). R_f = 0.30 (EtOAc/*n*-hexane, 1/3, v/v); ^{1}H NMR ($CDCl_3$) δ 5.40 (d, 1H, J = 10.2 Hz, NH), 5.38 (s, 1H, C^{4}H), 4.81 (dd, 1H, J = 5.0 and 10.2 Hz, C^{2}H), 4.65 (m, 1H, C^{1}H-menthol), 2.75 (m, 1H, C^{1}H), 2.18 (m, 1H, C^{5}H), 1.98 (s, 3H, CH_3-acetyl), 1.97/1.15 (2 × m, 2H, C^{6}H$_2$), 1.85/0.98 (2 × m, 2H, C^{6}H$_2$-menthol), 1.84 (m, 1H, C^2-CH-menthol), 1.70 (s, 3H, C^3-CH$_3$), 1.67/0.87 (2 × m, 2H, C^{4}H$_2$-menthol), 1.66/1.04 (2 × m, 2H, C^{3}H$_2$-menthol), 1.45 (m, 1H, C^{5}H-menthol), 1.41 (m, 1H, C^{2}H-menthol), 1.03 (d, 3H, J = 7.2 Hz, C^5-CH$_3$), 0.90/ 0.74 (2 × d, 6H, J = 6.9 Hz, CH$_3$-menthol), 0.90 (d, 3H, J = 7.2 Hz, C^5-CH$_3$-menthol); ^{13}C NMR ($CDCl_3$, HSQC) δ 132.2 (C^4); 75.1 (C^1-menthol); 47.6 (C^2); 46.9 (C^2-menthol); 44.6 (C^1); 40.5 (C^6-menthol); 34.5 (C^4-menthol); 31.7 (C^5-menthol); 30.9 (C^5); 29.0 (C^6); 26.7 (C^2-*C*H-menthol); 23.9 (C^3-menthol); 23.5 (CH$_3$-acetyl); 22.3 (C^5-*C*H$_3$-menthol); 21.8 (C^5-*C*H$_3$); 21.1 (CH$_3$-menthol); 21.0 (C^3-*C*H$_3$); 16.8 (CH$_3$-menthol); MS (ESI) *m*/*z* 350.2 [M + H]$^+$, 372.2 [M + Na]$^+$; HRMS (EI) calcd for $C_{21}H_{35}NO_3$ 349.2617, found 349.2616; RP-HPLC t_R = 17.8 (50−100%).

(b) [1*S*, 2*S*, 5*R*]-2-(Acetylamino)-3,5-dimethylcyclohex-3-enecarboxylic Acid (−)-8-Phenylmenthyl Ester (7b). R_f = 0.33 (EtOAc/*n*-hexane, 1/3, v/v); ^{1}H NMR ($CDCl_3$) δ 7.33−7.22 (m, 4H, Ar), 7.07 (t, 1H, J = 7 Hz, Ar), 5.29 (s, 1H, C^{4}H), 5.26 (d, 1H, J = 10.2 Hz, NH), 4.76 (m, 1H, C^{1}H-menthol), 4.33 (dd, 1H, J = 4.9 and 10.2 Hz, C^{2}H), 2.12 (m, 1H, C^{2}H-menthol), 1.99 (m, 1H, C^{5}H), 1.92 (s, 3H, CH$_3$-acetyl), 1.80/ 1.14 (2 × m, 2H, C^{3}H$_2$-menthol), 1.76/0.92 (2 × m, 2H, C^{6}H$_2$), 1.67/0.96 (2 × m, 2H, C^{6}H$_2$-menthol), 1.65/0.90 (2 × m, 2H, C^{4}H$_2$-menthol), 1.62 (m, 1H, C^{1}H), 1.60 (s, 3H, C^3-CH$_3$), 1.43 (m, 1H, C^{5}H-menthol), 1.29/1.18 (2 × s, 6H, CH$_3$-menthol), 0.99 (d, 3H, J = 7.2 Hz, C^5-CH$_3$), 0.87 (d, 3H, J = 7.2 Hz, C^5-CH$_3$-menthol); ^{13}C NMR ($CDCl_3$, HSQC) δ 132.0 (C^4), 128.1/125.7/ 125.2 (Ar), 74.7 (C^1-menthol), 50.3 (C^2-menthol), 47.6 (C^2), 44.0 (C^1), 41.3 (C^6-menthol), 34.8 (C^4-menthol), 31.7 (C^5-menthol), 30.7 (C^5), 29.9 (CH$_3$-menthol), 28.6 (C^6), 26.8 (C^3-menthol), 23.7 (CH$_3$-menthol), 23.5 (CH$_3$-acetyl), 22.1 (C^5-*C*H$_3$-menthol), 21.7 (C^5-*C*H$_3$), 20.9 (C^3-*C*H$_3$); MS (ESI) *m*/ *z* 426.2 [M + H]$^+$, 448.3 [M + Na]$^+$; HRMS (EI) calcd for $C_{21}H_{35}NO_3$ 425.2930, found 425.2932; RP-HPLC t_R = 19.8 (50−100%).

(c) [1*S*, 2*S*, 5*R*]-2-(Benzyloxy)carbonylamino-3,5-dimethylcyclohex-3-enecarboxylic Acid (−)-Menthyl Ester (7c). R_f = 0.25 (EtOAc/*n*-hexane, 1/10, v/v); ^{1}H NMR ($CDCl_3$) δ 7.41−7.23 (m, 5H, Ar), 5.35 (s, 1H, C^{4}H), 5.17/4.96 (2 × d, 2H, J = 12.2 Hz, CH$_2$-benzyl), 4.78 (d, 1H, J = 10.4 Hz, NH), 4.69 (m, 1H, C^{1}H-menthol), 4.50 (dd, 1H, J = 4.9 and 10.4 Hz, C^{2}H), 2.74 (m, 1H, C^{1}H), 2.14 (m, 1H, C^{5}H), 1.88/0.99 (2 × m, 2H, C^{6}H$_2$-menthol), 1.82 (m, 1H, C^2-CH-menthol), 1.79/1.10 (2 × m, 2H, C^{6}H$_2$), 1.70 (s, 3H, C^3-CH$_3$), 1.66/1.03 (2 × m, 2H, C^{3}H$_2$-menthol), 1.66/0.86 (2 × m, 2H, C^{4}H$_2$-menthol), 1.44 (m, 1H, C^{5}H-menthol), 1.39 (m, 1H, C^{2}H-menthol), 1.00 (d, 3H, J = 7.0 Hz, C^5-CH$_3$), 0.88/ 0.74 (2 × d, 6H, J = 6.9 Hz, CH$_3$-menthol), 0.86 (d, 3H, J = 7.2 Hz, C^5-CH$_3$-menthol); ^{13}C NMR ($CDCl_3$, HSQC) δ 132.0 (C^4), 129.3−127.4 (Ar), 75.2 (C^1-menthol), 67.4 (CH$_2$-benzyl), 50.0 (C^2), 47.2 (C^2-menthol), 45.0 (C^1), 40.4 (C^6-menthol), 34.5 (C^4-menthol), 31.8 (C^5-menthol), 30.9 (C^5), 28.8 (C^6), 26.6 (C^2-*C*H-menthol), 23.7 (C^3-menthol), 22.4 (C^5-*C*H$_3$-menthol), 21.8 (C^5-*C*H$_3$), 21.2 (CH$_3$-menthol), 21.0 (C^3-*C*H$_3$), 16.7 (CH$_3$-menthol); MS (ESI) *m*/*z* 442.2 [M + H]$^+$, 464.4 [M + Na]$^+$; HRMS (EI) calcd for $C_{21}H_{35}NO_3$ 441.2879, found 441.2877; RP-HPLC t_R = 26.6 (50−100%).

(d) [1*S*, 2*S*, 5*R*]-2-(Benzyloxy)carbonylamino-3,5-dimethylcyclohex-3-enecarboxylic Acid (−)-8-Phenylmenthyl Ester (7d). R_f = 0.32 (EtOAc/*n*-hexane, 1/10, v/v); ^{1}H NMR ($CDCl_3$) δ 7.34−7.23 (m, 9H, Ar), 7.07 (t, 1H, J = 7 Hz, CH−Ar), 5.24 (s, 1H, C^{4}H), 5.13/4.91 (2 × d, 2H, J = 12.2 Hz, CH$_2$-benzyl), 4.80 (m, 1H, C^{1}H-menthol), 4.49 (d, 1H, J = 10.6 Hz, NH), 4.00 (dd, 1H, J = 4.9 and 10.6 Hz, C^{2}H), 2.15 (m, 1H, C^{2}H-menthol), 1.97 (m, 1H, C^{5}H), 1.80/1.15 (2 × m, 2H, C^{3}H$_2$-menthol), 1.77/1.01 (2 × m, 2H, C^{6}H$_2$-menthol), 1.75/0.84 (2 × m, 2H, C^{6}H$_2$), 1.67/0.92 (2 × m, 2H, C^{4}H$_2$-menthol), 1.67 (m, 1H, C^{1}H), 1.63 (s, 3H, C^3-CH$_3$), 1.42 (m, 1H, C^{5}H-menthol), 1.31/1.19 (2 × s, 6H, CH$_3$-menthol), 0.96 (d, 3H, J = 7.2 Hz, C^5-CH$_3$), 0.83 (d, 3H, J = 7.2 Hz, C^5-CH$_3$-menthol); ^{13}C NMR ($CDCl_3$, HSQC) δ 131.5 (C^4), 129.1−124.8 (Ar), 74.5 (C^1-menthol), 67.0 (CH^2-benzyl), 50.2 (C^2-menthol), 49.5 (C^2), 44.3 (C^1), 41.0 (C^6-menthol), 34.7 (C^4-menthol), 31.6 (C^5-menthol), 30.6 (C^5), 29.5 (CH$_3$-menthol), 28.3 (C^6), 26.6 (C^3-menthol), 23.7 (CH$_3$-menthol), 22.2 (C^5-*C*H$_3$-menthol), 21.7 (C^5-*C*H$_3$), 20.9 (C^3-*C*H$_3$); MS (ESI) *m*/*z* 518.3 [M + H]$^+$, 540.4 [M + Na]$^+$; HRMS (EI) calcd for $C_{21}H_{35}NO_3$ 517.3192, found 517.3195; RP-HPLC t_R = 27.7 (50−100%).

(e) [1*S*, 2*S*, 5*R*]-2-(Benzyloxy)carbonylamino-3,5-dibenzylcyclohex-3-enecarboxylic Acid (−)-8-Phenylmenthyl Ester (7e). R_f = 0.25 (EtOAc/*n*-hexane, 1/10, v/v); ^{1}H NMR ($CDCl_3$) δ 7.41−6.87 (m, 20H, Ar), 5.37 (s, 1H, C^{4}H), 5.06/4.87 (2 × d, 2H, J = 12.2 Hz, CH$_2$-Z), 4.71 (m, 1H, C^{1}H-menthol), 4.40 (d, 1H, J = 10.6 Hz, NH), 4.06 (dd, 1H, J = 4.6 and 10.6 Hz, C^{2}H), 3.21 (s, 2H, C^3-CH$_2$), 2.60/2.51 (2 × dd, 2H, J = 7.2 and 13.5, C^5-CH$_2$), 2.18 (m, 1H, C^{5}H), 2.12 (m, 1H, C^{2}H-menthol), 1.81/1.13 (2 × m, 2H, C^{3}H$_2$-menthol), 1.73/0.97 (2 × m, 2H, C^{6}H$_2$-menthol), 1.70/ 0.94 (2 × m, 2H, C^{6}H$_2$), 1.64/0.90 (2 × m, 2H, C^{4}H$_2$-menthol), 1.46 (m, 1H, C^{1}H), 1.42 (m, 1H, C^{5}H-menthol), 1.22/1.12 (2 × s, 6H, CH$_3$-menthol), 0.80 (d, 3H, J = 7.2 Hz, C^5-CH$_3$-menthol); ^{13}C NMR ($CDCl_3$, HSQC) δ 130.8 (C^4), 130.2−124.5 (Ar), 74.6 (C^1-menthol), 67.2 (CH$_2$-Z), 50.1 (C^2-menthol), 48.5 (C^2), 44.1 (C^1), 42.8 (C^5-*C*H$_2$), 41.1 (C^3-*C*H$_3$), 41.0 (C^6-menthol), 37.8 (C^5), 34.8 (C^4-menthol), 30.6 (C^5-menthol), 30.1 (CH$_3$-menthol), 26.6 (C^3-menthol), 26.0 (C^6), 23.1 (CH$_3$-menthol), 22.1 (C^5-*C*H$_3$-menthol); MS (ESI) *m*/*z* 670.3 [M + H]$^+$, 692.4 [M + Na]$^+$; HRMS (EI) calcd for $C_{21}H_{35}NO_3$ 669.3818, found 669.3819; RP-HPLC t_R = 19.9 (80−100%).

(f) [1*S*, 2*S*, 5*R*]-3,5-Dimethyl-2-[*N*-((9*H*-fluoren-9-ylmethoxy)carbonyl)amino]cyclohex-3 -enecarboxylic Acid (8), Fmoc-cβAA-OH. A solution of **7d** (0.2 g, 0.39 mmol) in 12 mL of TFA and 1 mL of trifluoromethanesulfonic acid was stirred for 2 h at 0 °C. After evaporation of the solvent under reduced pressure, the remaining oil was dissolved in saturated $NaHCO_3$ solution (15 mL) and THF (10 mL) and Fmoc-ONSu (118 mg, 0.35 mmol) was added. The mixture was stirred for 10 h at room temperature and then adjusted to pH 2 by addition of 2 N HCl solution and the THF removed by evaporation under reduced pressure. The aqueous suspension was extracted with EtOAc (3 × 50 mL), the combined organic layers dried over $MgSO_4$, and the solvent evaporated under reduced pressure. Flash chromatography (EtOAc/*n*-hexane, 1/4, v/v, 1% AcOH) afforded **8** as white crystals (98 mg, 0.25 mmol, 64%): mp 78−80 °C (dec); R_f = 0.39 (EtOAc/*n*-hexane, 2/3, v/v, 1% AcOH); $[\alpha]^{25}_D$ −20° (2.0 mg/mL, H_2O) (without Fmoc); ^{1}H NMR ($CDCl_3$) δ 7.76 (t, 2 H, J = 7.6 Hz, Fmoc$_{Ar}$), 7.68 (t, 2 H, J = 7.6 Hz, Fmoc$_{Ar}$), 7.39 (t, 2 H, J = 7.6 Hz, Fmoc$_{Ar}$), 7.31 (t, 2 H, J = 7.6 Hz, Fmoc$_{Ar}$), 5.40 (s, 1 H, C^{4}H), 4.68 (d, 1 H, J = 10.6 Hz, HN), 4.52/4.38 (2 × m, 2 H, Fmoc-CH$_2$), 4.51 (dd, 1 H, J = 4.9 and 10.6 Hz, C^{2}H), 4.21 (m, 1 H, Fmoc-CH), 2.74 (m, 1 H, C^{1}H), 2.14 (m, 1 H, C^{5}H), 1.97/1.16 (2 × m, 2 H, C^{6}H$_2$), 1.69 (s, 3 H, CH$_3$), 1.03 (d, 3 H, J = 6.9 Hz, C^5-CH$_3$); ^{13}C NMR ($CDCl_3$) δ 172.8 (CO), 156.1 (CO$_{Fmoc}$), 143.4 (Fmoc), 141.1 (Fmoc), 132.0 (C^3), 131.8 (C^4), 127.5 (Fmoc$_{Ar}$), 126.8 (Fmoc$_{Ar}$), 124.9 (Fmoc$_{Ar}$), 119.7 (Fmoc$_{Ar}$), 66.4 (Fmoc-CH$_2$), 49.4 (C^2), 47.2 (Fmoc-CH), 43.7 (C^1), 30.3 (C^5), 27.8 (C^6), 21.1 (C^5-*C*H$_3$), 20.8 (CH$_3$); MS (ESI) *m*/*z* 392.2 [M + H]$^+$, 414.2 [M + Na]$^+$, 805.2 [2M + Na]$^+$, 821.3 [2M + K]$^+$, 1196.2 [3M + Na]$^+$, 1212.1 [3M + K]$^+$; HRMS (EI) calcd for $C_{24}H_{25}NO_4$ 391.1784, found 391.1785; RP-HPLC t_R = 25.2 (10−90%).

Solid-Phase Peptide Synthesis and Purification. Peptide synthesis was carried out using TCP resin following standard Fmoc strategy.[37] Side chain unprotected Fmoc-Tyr-OH (97 mg, 0.24 mmol) was attached to the TCP resin (0.20 g) with DIEA (100 μL) in anhydrous DCM (2 mL) at room temperature for 1 h, followed by addition of MeOH (0.2 mL) for 15 min for quenching, yielding 0.24 g of Fmoc-Tyr-TCP-resin (substitution level 0.43 mmol/(g of resin)). For Fmoc deprotection the resin was treated with 20% piperidine in NMP (v/v) and washed with NMP. The coupling of 1.8 equiv of Fmoc-cβAA-OH (**8**; 60 mg, 15 mmol) was achieved using TBTU (49 mg, 15 mmol), HOBt (24 mg, 16 mmol), DIEA (72 μL), in NMP (2 mL) for 2 h at room temperature. For attachment of (*S*)-/

(*R*)-Mosher acid to the unprotected N-terminus of the cβAA-Tyr dipeptide, 60 mg of NH_2-cβAA-Tyr-TCP-resin (approximately 27 μmol) was treated with 5.0 equiv of (*R*)- or (*S*)-Mosher acid chloride (34 mg, 0.14 mmol) and collidine (40 μL) in dry DMF for 1 h at room temperature. The Mosher amides **11a**,**b** were cleaved from resin by treatment with 20% HFIP in DCM (v/v) for 15 min and purified by preparative RP-HPLC (>98% purity).

(a) (*S*)-Mosher Amide of H_2N-cβAA-Tyr-OH (11a). ^{1}H NMR (DMSO-d_6) δ 9.13 (bs, 1H, OH), 8.08 (d, 1H, J = 8.0 Hz, HN-Tyr), 7.49 (d, 1H, J = 9.7 Hz, HN-cβAA), 7.36−7.46 (m, 5H, Mosher$_{Ar}$), 6.93/6.62 (2 × d, 4H, J = 8.4 Hz, Tyr$_{Ar}$), 5.38 (s, 1H, C^{4}H), 4.64 (dd, 1H, J = 4.7 and 9.7 Hz, C^{2}H), 4.39 (m, 1H, H$^\alpha$), 3.13 (s, 3H, MeO), 2.88/2.72 (2 × dd, 2H, ^2J = 14 Hz, ^3J = 5.4 and 7.5 Hz, H$^\beta$), 2.71 (m, 1H, C^{1}H), 2.09 (m, 1H, C^{5}H), 1.61 (s, 3H, CH$_3$), 1.49/1.34 (2 × m, 2H, C^{6}H$_2$), 0.96 (d, 3H, J = 7.0 Hz, C^5-CH$_3$); ^{13}C NMR (DMSO-d_6) δ 172.8 (CO-Tyr), 171.9 (CO-cβAA), 164.9 (CO−Mosher), 156.1 (C$_q$-Tyr), 132.0 (C^3), 131.8 (C^4), 131.6 (C$_q$-Mosher), 130.4 (Tyr$_{Ar}$), 129.7 (Mosher$_{Ar}$), 128.9 (Mosher$_{Ar}$), 128.6 (Mosher$_{Ar}$), 127.6 (C$_q$-Tyr), 124.3 (CF$_3$), 115.1 (Tyr$_{Ar}$), 84.2 (C−CF$_3$), 54.7 (MeO), 53.7 (C$^\alpha$), 47.9 (C^2), 43.9 (C^1), 37.3 (C$^\beta$), 30.6 (C^5), 28.7 (C^6), 21.3 (CH$_3$), 20.8 (C^3-*C*H$_3$); MS (ESI) *m/z* 549.3 [M + H]$^+$, 571.4 [M + Na]$^+$, 1119.3 [2M + Na]$^+$; RP-HPLC t_R = 22.4 (10−90%).

(b) (*R*)−Mosher Amide of H_2N-cβAA-Tyr-OH (11b). ^{1}H NMR (DMSO-d_6) δ 9.14 (s, 1H, OH), 7.96 (d, 1H, J = 7.8 Hz, HN-Tyr), 7.55 (d, 1H, J = 9.5 Hz, NH-cβAA), 7.52/7.39 (2 × m, 5H, Mosher$_{Ar}$), 6.95/6.63 (2 × d, 4H, J = 8.4 Hz, Tyr$_{Ar}$), 5.23 (s, 1H, C^{4}H), 4.64 (dd, 1H, J = 4.3 and 9.3 Hz, C^{2}H), 4.28 (m, 1H, H$^\alpha$), 3.48 (s, 3H, MeO), 2.91/2.73 (2 × dd, 2H, ^2J = 13.8 Hz, ^3J = 5.8 and 7.3 Hz, H$^\beta$), 2.62 (m, 1H, C^{1}H), 2.02 (m, 1H, C^{5}H), 1.50/1.38 (2 × m, 2H, C^{6}H$_2$), 1.39 (s, 3H, CH$_3$), 0.86 (d, 3H, J = 7.1 Hz, C^5-CH$_3$); ^{13}C NMR (DMSO-d_6) δ 172.8 (CO-Tyr), 172.2 (CO-cβAA), 165.4 (CO−Mosher), 156.2 (C$_q$-Tyr), 134.3 (C$_q$-Mosher), 131.8 (C^3), 131.6 (C^4), 130.4 (Tyr$_{Ar}$), 129.5 (Mosher$_{Ar}$), 128.4 (Mosher$_{Ar}$), 127.8 (C$_q$-Tyr), 127.1 (Mosher$_{Ar}$), 124.3 (CF$_3$), 115.1 (Tyr$_{Ar}$), 83.6 (C−CF$_3$), 55.6 (MeO), 54.0 (C$^\alpha$), 48.2 (C^2), 44.1 (C^1), 37.0 (C$^\beta$), 30.6 (C^5), 28.3 (C^6), 21.0 (CH$_3$), 21.0 (C^3-*C*H$_3$); MS (ESI) *m/z* 549.3 [M + H]$^+$, 571.4 [M + Na]$^+$, 1119.3 [2M + Na]$^+$; RP-HPLC t_R = 22.1 (10−90%).

Elongation of the peptide chain for synthesis of cyclic peptides **2a,b** and **3a**−**c** was done using 3.0 equiv of Fmoc-Pro-OH, Fmoc-Phe-OH, Fmoc-Thr(Trt)-OH, Fmoc-Nle-OH, and Fmoc-D-Trp-OH each and proportionally higher amounts of TBTU, HOBt, and DIEA, respectively. Before cleavage of the partly protected linear peptides from its resin support, the Fmoc protection was removed. After washings with DCM, the peptides were cleaved from resin with a mixture of AcOH, TFE, and DCM (2/1/6, v/v/v) for 1 h at room temperature. After evaporation of the solvents, the crude linear peptides were cyclized without further purification. For cyclization, the linear fragments were dissolved in DMF to a concentration of 4 mM, treated with 3 equiv of HOBt, 5 equiv of collidine, and 1.2 equiv of PyBOP and stirred 16 h at room temperature until completion. The solvent was almost completely removed in vacuo, and the products were then precipitated with ether and dried. Preparative HPLC purification (mobile phase H_2O/ACN, no TFA) afforded Trt protected peptides **2b** and **3b**,**c**. For complete deprotection, the peptides **2b** and **3b** were dissolved at 0 °C in TFA/TIS/DMC (2/1/97, v/v/v) and the mixture was stirred for 1 h in the cold. After evaporation of the solvent the products were precipitated with ether and dried. Preparative HPLC purification afforded fully deprotected peptides **2a** and **3a**.

Cyclo[Pro-Tyr-D-Trp-Nle-Thr-Phe] (**2a**): 98% purity; RP-HPLC t_{R1} = 17.38 (20−80%) t_{R2} = 17.41 (10−100%); MS (ESI) *m/z* 808.5 [M + H]$^+$, 830.6 [M + Na]$^+$.

Cyclo[Pro-Tyr-D-Trp-Nle-Thr(Trt)-Phe] (**2b**): 97% purity; RP-HPLC t_{R1} = 11.69 (60−100%), t_{R2} = 26.01 (10−100%); MS (ESI) *m/z* 1072.6 [M + Na]$^+$, 808.6 [M − Trt + H]$^+$.

Cyclo[cβAA-Tyr-D-Trp-Nle-Thr] (**3a**): 97% purity (determined by HPLC and ^{1}H NMR); RP-HPLC t_{R1} = 18.27 (10−90%); MS (ESI) *m/z* 715.4 [M + H]$^+$, 737.5 [M + Na]$^+$.

Cyclo[cβAA-Tyr-D-Trp-Nle-Thr(Trt)] (**3b**): 98% purity (determined by HPLC and ^{1}H NMR); RP-HPLC t_{R1} = 29.18 (10−90%); MS (ESI) *m/z* 979.5 [M + Na]$^+$, 715.4 [M − Trt + H]$^+$.

Cyclo[cβAA-D-Tyr-D-Trp-Nle-Thr(Trt)] (**3c**): 95% purity (determined by HPLC and ^{1}H NMR); RP-HPLC t_{R1} = 28.82 (10−90%), MS (ESI) *m/z* 979.4 [M + Na]$^+$, 715.4 [M − Trt + H]$^+$.

Biological Assay. Human A431 epidermoid carcinoma cells were cultures in DMEM (Dulbecco's Mod Eagle Medium) supplemented with 10% FCS (fetal calf serum), 200 mM L-glutamine, 10 000 U/mL penicillin, and 10 mg/mL streptomycin (Gibco Life Sci) at 37 °C and 5% CO_2. Cells were seeded in 96-well plates and incubated for 16 h before serial dilutions of compounds were added. Cells were treated for 6 and 48 h. Cells used for 6 and 48 h treatments were seeded at 4 × 10^4 and 1 × 10^4 per well, respectively. Antiproliferative efficacy of the compounds was analyzed with methylene blue test.

All compounds were dissolved in DMSO and diluted in cell culture medium for the proliferation test in final concentrations of 50, 10, 2, 0.4, and 0.08 μM and tested in duplicate. Cycloheximide, a well-established inducer of apoptosis, was used as positive control.

Antiproliferative effect was first expressed as a percentage of the optical density (OD) of treated (T) and negative control (D) wells after both 6 and 48 h (T/C × 100). Because new protein synthesis is required for apoptosis in immortalized cell lines, compounds that induce programmed cell death will show significantly less antiproliferative activity after 6 h than after 48 h. In the optimal case an apoptosis-inducing compound will cause 100% viability after 6 h and 0% after 48 h. Therefore, analyzing T/C_{48h} versus T/C_{6h} will correlate with the apoptosis-inducing "specific" of a compound. The cutoff limit for "effective" compounds was set for differences expressed as (T/C_{6h} − T/C_{48h}) > 80%. IC_{50} values were generated from IC_{50} graphs.

NMR Spectroscopy of Peptides. The spectra were recorded at 300 K on a Bruker DMX spectrometer operating at 500 MHz. The samples were prepared in DMSO-d_6 at a concentration of 1.5−3 mM. DMSO-d_6 was used as an internal standard (2.49 ppm for ^{1}H and 39.5 ppm for ^{13}C). $J_{H,H}$ coupling constants and amide hydrogen temperature coefficients were measured from 1D experiments carried out at 295, 300, 305, 310, and 315 K. The data were processed with XWINNMR 3.5 software from Bruker. Homo- and heteronuclear experiments DQF−COSY, TOCSY, ROESY, and HSQC were performed with a spectral width of 12 ppm for ^{1}H and 150 ppm for ^{13}C. In all of the experiments, spectra were recorded with 1024 increments in t_1 and 4096 complex data points in t_2. For ROESY, 32 transients were averaged for each t_1 value; for COSY, ^{13}C-HSQC, and TOCSY, 16 transients. A mixing time of 70 or 250 ms was used for TOCSY (spin lock field, 10 kHz; mixing sequence, MLEV-17) and ROESY spectra, respectively. Water signal suppression was achieved by WATERGATE (W5) techniques.[44] Sequential assignment and quantitative information on interproton distances were obtained from ROESY spectra (250 ms mixing time; spin lock field, 5.00 kHz). The volume integrals of the individually assigned cross-peaks were converted into distance constraints using the isolated spin pair approximation[45] and taking the offset effect into account. The ROESY cross-peak volumes were calibrated against the distance (1.78 Å) between the prochiral H^6 methylene protons of cβAA.

Upper and lower distance limits were set to plus and minus 10% of the calculated distances, respectively. For nondiastereotopically assigned methyl groups, 0.9 Å were added to the upper bounds as pseudoatom corrections, respectively.

Molecular Modeling. The structural NMR refinement protocol included distance geometry, energy minimizations, and molecular dynamics (MD) simulations. A modified version of the distance geometry (DG) program DISGEO[46,47] was used to generate structures consistent with 35 distance constraints derived from ROEs. The DG procedure started with the embedding of 100 structures using random metrization. The structure with the smallest total error was placed in a cubic box with a box length of 40 Å and soaked with DMSO.[40] The

MD calculations were carried out employing the module DISCOVER of the INSIGHT II 2001 program (Biosym/MSI Inc.) with the CVFF force field, and the ROE restraints were included with a force constant of 10 kcal/(mol Å^2). The calculations were done with the explicit-image model of periodic boundary conditions. After energy minimization using the steepest descent and conjugate gradient, the system was heated gradually starting from 10 K and increasing to 50, 100, 150, 200, 250, and 300 K in 1 ps steps, each by direct scaling of velocities. Configurations were saved every 100 fs for another 150 ps. The averaged structure of the restrained MD was minimized by using the method of steepest descent. Distance violations were calculated by $\langle r^{-3} \rangle^{-1/3}$ averaging. The MD calculation was continued without restraints for another 150 ps with an unchanged sampling rate.

Acknowledgment. The authors gratefully acknowledge technical assistance from M. Kranawitter, B. Cordes, and M. Wolff. We would like to thank J. Krause for the EI-HRMS analyses of the intermediates. E.B. thanks the Fonds FQRNT of Quebec and the Foundation Alexander von Humboldt for Postdoctoral Fellowships. Financial support was provided by the Deutsche Forschungsgemeinschaft and the Fonds der Chemischen Industrie, as well as grants from the Hungarian Ministry of Education KKK-01/2001, NKFP-21/2002, and OTK 49478.

Appendix

Abbreviations. All optically active amino acids are of the L variety unless otherwise stated. Other abbreviations are the following: Bzl, benzyl; cβAA, cyclic β-amino acid; $CDCl_3$, deuterated chloroform; COSY, correlation spectroscopy; DG, distance geometry; DIEA, diisopropylethylamine; DMF, dimethylformamide; DMSO-d_6, fully deuterated dimethyl sulfoxide; FACS, fluorescence activated cell sorter; Fmoc, fluorenylmethoxycarbonyl; Fmoc-ONSu, (9-fluorenylmethoxycarbonyloxy) succinimide; HOBt, 1-hydroxybenzotriazole; HSQC, heteronuclear single quantum coherence; MD, molecular dynamics; NMP, *N*-methylpyrrolidinone; PyBOP, benzotriazol-1-yloxytrispyrrolidinophosphonium hexafluorophosphate; rmsd, root-mean-square deviation; ROESY, rotating frame nuclear Overhauser spectroscopy; RP-HPLC, reverse-phase high-performance liquid chromatography; TBTU, *O*-(benzotriazol-1-yl)-*N*,*N*,*N*′,*N*′-tetramethyluronium tetrafluoroborate; TCP, trityl chloride polystyrol; TFA, trifluoroacetic acid; TFE, 2,2,2-trifluoroethanol; TIS, triisopropylsilane; TOCSY, total correlation spectroscopy; Trt, triphenylmethyl; Z, benzyloxycarbonyl.

Supporting Information Available: Distance restraints and their violations from the 150 ps restrained MD simulation of peptide **3b**, proton and carbon chemical shifts of peptide **3b** and temperature coefficients for the amide protons, and $^3J_{H,H}$ coupling constants of amide and side chain protons of peptide **3b**. This material is available free of charge via Internet at http://pubs.acs.org.

References

(1) Brazeau, P.; Vale, W.; Burgus, R.; Ling, N.; Butcher, M.; Rivier, J.; Guillemin, R. Hypothalamic Polypeptide That Inhibits the Secretion of Immunoreactive Pituitary Growth Hormone. *Science* **1973**, *179*, 77−79.

(2) Koerker, D. J.; Harker, L. A.; Goodner, C. J. Effects of Somatostatin on Hemostasis in Baboons. *N. Engl. J. Med.* **1975**, *293*, 476−479.

(3) Gerich, J. E.; Lovinger, R.; Grodsky, G. M. Inhibition by Somatostatin of Glucagon and Insulin Release from the Perfused Rat Pancreas in Response to Arginine, Isoproterenol and Theophylline: Evidence for a Preferential Effect on Glucagon Secretion. *Endocrinology* **1975**, *96*, 749−754.

(4) Johansson, C.; Wisen, O.; Efendic, S.; Uvnas-Wallensten, K. Effects of Somatostatin on Gastrointestinal Propagation and Absorption of Oral Glucose in Man. *Digestion* **1981**, *22*, 126−137.

(5) Patel, Y. C. Somatostatin and Its Receptor Family. *Front. Neuroendocrinol.* **1999**, *20*, 157−198.

(6) Froidevaux, S.; Eberle, A. N. Somatostatin Analogues and Radiopeptides in Cancer Therapy. *Biopolymers* **2002**, *66*, 161−183.

(7) Bruns, C.; Raulf, F.; Hoyer, D.; Schloos, J.; Lübbert, H.; Weckbecker, G. Binding Properties of Somatostatin Receptor Subtypes. *Metabolism* **1996**, *45*, 17−20.

(8) Weckbecker, G.; Lewis, I.; Albert, R.; Schmid, H. A.; Hoer, D.; Bruns, C. Opportunities in Somatostatin Research: Biological, Chemical and Therapeutic Aspects. *Nat. Rev. Drug Discovery* **2003**, *2*, 999−1017.

(9) Gademann, K.; Ernst, M.; Seebach, D.; Hoyer, D. The Cyclo-beta-Tetrapeptide (beta-HPhe-beta-HThr-beta-HLys-beta-HTrp): Synthesis, NMR Structure in Methanol Solution, and Affinity for Human Somatostatin Receptors. *Helv. Chim. Acta* **2000**, *83*, 16−33.

(10) Veber, D. F.; Freidlinger, R. M.; Perlow, D. S.; Paleveda, W. J., Jr.; Holly, F. W.; Strachan, R. G.; Nutt, R. F.; Arison, B. H.; Homnick, C.; Randall, W. C.; Glitzer, M. S.; Saperstein, R.; Hirschmann, R. A Potent Cyclic Hexapeptide Analogue of Somatostatin. *Nature* **1981**, *292*, 55−58.

(11) Veber, D. F.; Saperstein, R.; Nutt, R. F.; Freidinger, R. M.; Brady, S. F.; Curley, P.; Perlow, D. S.; Paleveda, W. J.; Colton, C. D.; Zacchei, A. G.; Tocco, D. J.; Hoff, D. R.; Vandlen, R. L.; Gerich, J. E.; Hall, L.; Mandarino, L.; Cordes, E. H.; Anderson, P. S.; Hirschmann, R. A Super Active Cyclic Hexapeptide Analogue of Somatostatin. *Life Sci.* **1984**, *34*, 1371−1378.

(12) Freidinger, R. M.; Perlow, D. S.; Randall, W. C.; Saperstein, R.; Arison, B. H.; Veber, D. F. Conformational Modifications of Cyclic Hexapeptide Somatostatin Analogues. *Int. J. Pept. Protein Res.* **1984**, *23*, 142−150.

(13) Nutt, R. F.; Veber, D. F.; Curley, P. E.; Saperstein, R.; Hirschmann, R. Somatostatin Analogues Which Define the Role of the Lysine-9 Amino Group. *Int. J. Pept. Protein Res.* **1983**, *21*, 66−73.

(14) Schally, A. V. Oncological Applications of Somatostatin Analogues. *Cancer Res.* **1988**, *48*, 6977−6985.

(15) Logothetis, C. J.; Hossan, E. A.; Smith, T. L. SMS 201-995 in the Treatment of Refractory Prostatic Carcinoma. *Anticancer Res.* **1994**, *14*, 2731−2734.

(16) Kessler, H.; Bernd, M.; Kogler, H.; Zarbock, J.; Soerensen, O. W.; Bodenhausen, G.; Ernst, R. R. Peptide Conformations. 28. Relayed Heteronuclear Correlation Spectroscopy and Conformational Analysis of Cyclic Hexapeptides Containing the Active Sequence of Somatostatin. *J. Am. Chem. Soc.* **1983**, *105*, 6944−6952.

(17) Mierke, D. F.; Pattaroni, C.; Delaet, N.; Toy, A.; Goodman, M.; Tancredi, T.; Motta, A.; Temussi, P. A.; Moroder, L.; Bovermann, G.; Wunsch, E. Cyclic Hexapeptides Related to Somatostatin—Conformational Analysis Employing Proton NMR and Molecular Dynamics. *Int. J. Pept. Protein Res.* **1990**, *36*, 418−432.

(18) Huang, Z. W.; He, Y. B.; Raynor, K.; Tallent, M.; Reisine, T.; Goodman, M. Main Chain and Side-Chain Chiral Methylated Somatostatin Analogs: Syntheses and Conformational Analyses. *J. Am. Chem. Soc.* **1992**, *114*, 9390−9401.

(19) He, Y. B.; Huang, Z. W.; Raynor, K.; Reisine, T.; Goodman, M. Synthesis and Conformations of Somatostatin-Related Cyclic Hexapeptides Incorporating Specific α- and β-Methylated Residues. *J. Am. Chem. Soc.* **1993**, *115*, 8066−8072.

(20) Hirschmann, R.; Nicolaou, K. C.; Pietranico, S.; Leahy, E. M.; Salvino, J. Arison, B.; Cichy, M. A.; Spoors, P. G.; Shakespeare, W. C.; Sprengeler, P. A.; Hamley, P.; Smith, A. B.; Reisine, T.; Raynor, K.; Maechler, L.; Donaldson, C.; Vale, W.; Freidinger, R. M.; Cascieri, M. R.; Strader, C. D. De Novo Design and Synthesis of Somatostatin Non-peptide Peptidomimetics Utilizing β-D-Glucose as a Novel Scaffolding. *J. Am. Chem. Soc.* **1993**, *115*, 12550−12568.

(21) Pattaroni, C.; Lucietto, P.; Goodman, M.; Yamamoto, G.; Vale, W.; Moroder, L.; Gazerro, L.; Gohring, W.; Schmied, B.; Wunsch, E. Cyclic Hexapeptides Related to Somatostatin—Synthesis and Biological Testing. *Int. J. Pept. Protein Res.* **1990**, *36*, 401−417.

(22) Rohrer, S. P.; Birzin, E. T.; Mosley, R. T.; Berk, S. C.; Hutchins, S. M.; Shen, D. M.; Xiong, Y. S.; Hayes, E. C.; Parmar, R. M.; Foor, F.; Mitra, S. W.; Degrado, S. J.; Shu, M.; Klopp, J. M.; Cai, S. J.; Blake, A.; Chan, W. W. S.; Pasternak, A.; Yang, L. H.; Patchett, A. A.; Smith, R. G.; Chapman, K. T.; Schaeffer, J. M. Rapid Identification of Subtype-Selective Agonists of the Somatostatin Receptor through Combinatorial Chemistry. *Science* **1998**, *282*, 737−740.

(23) Keri, G.; Erchegyi, J.; Horvath, A.; Mezo, I.; Idei, M.; Vantus, T.; Balogh, A.; Vadasz, Z.; Bokonyi, G.; Seprodi, J.; Teplan, I.; Csuka, O.; Tejeda, M.; Gaal, D.; Szegedi, Z.; Szende, B.; Roze, C.; Kalthoff, H.; Ullrich, A. A Tumor-Selective Somatostatin Analogue (TT-232) with Strong in Vitro and in Vivo Antitumor Activity. *Proc. Natl. Acad. Sci. U.S.A.* **1996**, *93*, 12513−12518.
(24) Vantus, T.; Keri, G.; Krivickiene, Z.; Valius, M.; Stetak, A.; Keppens, S.; Csermely, P.; Bauer, P. I.; Bokonyi, G.; Declercq, W.; Vandenabeele, P.; Merlevede, W.; Vandenheede, J. R. The Somatostatin Analogue TT-232 Induces Apoptosis in A431 Cells—Sustained Activation of Stress-Activated Kinases and Inhibition of Signaling to Extracellular Signal-Regulated Kinases. *Cell. Signalling* **2001**, *13*, 717−725.
(25) Szegedi, Z.; Takacs, J.; Szende, B.; Vadasz, Z.; Horvath, A.; Gulyas, E.; Toth, G.; Petak, I.; Bocsi, J.; Keri, G. A Specifically Radiolabeled Somatostatin Analogue with Strong Antitumor Activity Induces Apoptosis and Accumulates in the Cytosol and the Nucleus of HT29 Human Colon Carcinoma Cells. *Endocrine* **1999**, *10*, 25−34.
(26) Li, H.; Jiang, X.; Howell, S. B.; Goodman, M. Synthesis, Conformational Analysis and Bioactivity of Lan-7, a Lanthionine Analogue of TT-232. *J. Pept. Sci.* **2000**, *6*, 26−35.
(27) Riniker, B.; Schwyzer, R. Synthetic Analogues of Hypertensin. V. α-L-, β-L-, α-D-, and β-D-Asp1-Val5-Hypertensin II; Deamino-Val5-Hypertensin II. *Helv. Chim. Acta* **1964**, *47*, 2357−2374.
(28) Ondetti, M. A.; Engel, S. L. Bradykinin Analogues Containing β-Homoamino Acids. *J. Med. Chem.* **1975**, *18*, 761−763.
(29) Seebach, D.; Albert, M.; Arvidsson, P. I.; Rueping, M.; Schreiber, J. V. From the Biopolymer PHB to Biological Investigations of Unnatural beta- and gamma-Peptides. *Chimia* **2001**, *55*, 345−353.
(30) Gruner, S. A. Dissertation, Technical University Munich, Germany, 2002.
(31) Gruner, S. A.; Keri, G.; Schwab, R.; Venetianer, A.; Kessler, H. Sugar Amino Acid Containing Somatostatin Analogues That Induce Apoptosis in Both Drug-Sensitive and Multidrug-Resistant Tumor Cells. *Org. Lett.* **2001**, *3*, 3723−3725.
(32) Neumann, H.; von Wangelin, A. J.; Gordes, D.; Spannenberg, A.; Beller, M. A New Multicomponent Coupling of Aldehydes, Amides, and Dienophiles: Atom-Efficient One-Pot Synthesis of Highly Substituted Cyclohexenes and Cyclohexadienes. *J. Am. Chem. Soc.* **2001**, *123*, 8398−8399.
(33) Corey, E. J.; Ensley, H. E. Preparation of an Optically-Active Prostaglandin Intermediate via Asymmetric Induction. *J. Am. Chem. Soc.* **1975**, *97*, 6908−6909.
(34) de Pascual-Teresa, B.; Gonzalez, J.; Asensio, A.; Houk, K. N. Ab Initio-Based Force Field Modeling of the Transition States and Stereoselectivities of Lewis Acid-Catalyzed Asymmetric Diels−Alder Reactions. *J. Am. Chem. Soc.* **1995**, *117*, 4347−4356.
(35) Yajima, H.; Futaki, S.; Otaka, A.; Yamashita, T.; Funakoshi, S.; Bessho, K.; Fujii, N.; Akaji, K. Studies on Peptides: 143. Evaluation of beta-Menthylaspartate for Peptide Synthesis. *Chem. Pharm. Bull.* **1986**, *34*, 4356−4361.
(36) Ohtani, I.; Kusumi, T.; Kashman, Y.; Kakisawa, H. High-Field FT NMR Application of Mosher's Method: The Absolute Configurations of Marine Terpenoids. *J. Am. Chem. Soc.* **1991**, *113*, 4092−4096.
(37) Fields, G. B.; Noble, R. L. Solid-Phase Peptide Synthesis Utilizing 9-Fluorenylmethoxycarbonyl Amino Acids. *Int. J. Pept. Protein Res.* **1990**, *35*, 161−214.
(38) Kessler, H. Conformation and Biological Activity of Cyclic Peptides. *Angew. Chem., Int. Ed. Engl.* **1982**, *21*, 512−523.
(39) Kessler, H.; Seip, S. *NMR of Peptides*; VCH.: Weinheim, Germany, 1994; pp 619−654.
(40) Mierke, D. F.; Kessler, H. Molecular Dynamics with Dimethyl Sulfoxide as a Solvent. Conformation of a Cyclic Hexapeptide. *J. Am. Chem. Soc.* **1991**, *113*, 9466−9470.
(41) Flohr, S.; Kurz, M.; Kostenis, E.; Brkovich, A.; Fournier, A.; Klabunde, T. Identification of Nonpeptidic Urotensin II Receptor Antagonists by Virtual Screening Based on a Pharmacophore Model Derived from Structure−Activity Relationships and Nuclear Magnetic Resonance Studies on Urotensin II. *J. Med. Chem.* **2002**, *45*, 1799−1805.
(42) Rew, Y.; Malkmus, S.; Svensson, C.; Yaksh, T. L.; Chung, N. N.; Schiller, P. W.; Cassel, J. A.; DeHaven, R. N.; Goodman, M. Synthesis and Biological Activities of Cyclic Lanthionine Enkephalin Analogues: δ-Opioid Receptor Selective Ligands. *J. Med. Chem.* **2002**, *45*, 3746−3754.
(43) Jaspers, H.; Horvath, A.; Mezo, I.; Keri, G.; Vanbinst, G. Conformational Study of a Series of Somatostatin Analogues with Antitumor and/or GH Inhibitory Activity. *Int. J. Pept. Protein Res.* **1994**, *43*, 271−276.
(44) Liu, M.; Mao, X.-A.; Ye, C.; Huang, H.; Nicholson, J. K.; Lindon, J. C. Improved WATERGATE Pulse Sequences for Solvent Suppression in NMR Spectroscopy. *J. Magn. Reson.* **1998**, *132*, 125−129.
(45) Kumar, A.; Wagner, G.; Ernst, R. R.; Wüthrich, K. Buildup Rates of the Nuclear Overhauser Effect Measured by Two-Dimensional Proton Magnetic Resonance Spectroscopy: Implications for Studies of Protein Conformation. *J. Am. Chem. Soc.* **1981**, *103*, 3654−3658.
(46) Mierke, D. F.; Kessler, H. Improved Molecular Dynamics Simulations for the Determination of Peptide Structures. *Biopolymers* **1993**, *33*, 1003−1017.
(47) Havel, T. F. An Evaluation of Computational Strategies for Use in the Determination of Protein Structure from Distance Constraints Obtained by Nuclear Magnetic Resonance. *Prog. Biophys. Mol. Biol.* **1991**, *56*, 43−78.

JM049500J